NMR studies of vacancy motion in solid hydrogen

D. Zhou, M. Rall, J. P. Brison,* and N. S. Sullivan
Department of Physics, University of Florida, Gainesville, Florida 32611-2085
(Received 14 February 1990)

The temperature dependence of the nuclear-spin-lattice relaxation time of ortho-H_2 and HD impurities in solid parahydrogen has been studied from the melting point to 1.5 K. Three distinct temperature regimes are observed: (1) an exponential temperature dependence for 11 K $< T <$ 13.5 K, (2) a minimum for the relaxation time for 7 K $< T <$ 11 K, and (3) a weak, approximately linear dependence for 1.5 K $< T <$ 7 K. The overall behavior can be understood in terms of the cross relaxation between two weakly coupled energy reservoirs corresponding to the ortho-H_2 and HD impurities, respectively. The temperature dependence near the minimum is different from that at high temperatures and is interpreted as evidence for quantum tunneling of vacancies in the intermediate-temperature regime.

I. INTRODUCTION

The study of vacancies and other point defects in solids is important because of the insight that can be gained concerning the fundamental properties of the solids, (binding forces, atomic mobilities, diffusion, etc.), and also because of the profound influence defects can have on technologically important materials.[1-3] Vacancies and interstitials are point defects consisting of the absence of atoms (or the presence of additional atoms) and they are entirely responsible for the electrical conductivity in ionic crystals and can dramatically alter the optical properties (in particular, the color) of such solids. Other types of imperfections, such as dislocations which are irregularities involving lines and planes of atoms, play a major role in crystal growth and the mechanical strength of materials. The process of annealing and corresponding reduction of line and surface defects to their equilibrium value depends crucially on the properties of vacancies and their diffusion in the solid at different temperatures.

Qualitatively new effects have been predicted[4-8] for the behavior of vacancies and other point defects in the so-called quantum crystals such as solid helium and solid hydrogen, and considerable effort,[9-31] both experimental and theoretical, has been devoted to their study in recent years. In these quantum solids, there is a relatively large zero-point motion of the atoms or molecules about their equilibrium positions, 33% of the lattice spacing for solid ^{3}He and 18% in solid H_2. There is an appreciable overlap of the wave functions of the particles on neighboring lattice sites, and this allows defects such as vacancies or isotopic impurities to exchange position with nearest-neighbor atoms (or molecules). Whereas in the classical solids, the defects can be regarded as localized objects which move only occasionally by thermal excitation over intervening potential energy barriers, the defects will become delocalized in the quantum solids, and Andreev[4] has predicted that they will move through the crystal in a coherent manner by quantum tunneling. These excitations are called vacancy waves or impurity waves.[5,6]

The purpose of this paper is to discuss recent results of NMR studies of vacancies in solid H_2.[30,31] The possibility of observing quantum tunneling in solid H_2 is especially interesting, because there are two "bound" states for the molecule-vacancy interaction potential[23] (Fig. 1) and one can expect to observe three distinct temperature regimes for vacancy-induced diffusion:[30] (1) thermal activation over the full potential barrier at high for 11 K $< T <$ 14 K, (2) tunneling combined with thermal activation from the ground state on one side of the well to the first excited state on the other side of the well at intermediate temperatures (7 K $< T <$ 11 K, and (3) purely quantum tunneling through the potential barrier from ground state to ground state at low temperatures ($T \leq 7$ K). Each regime is expected to be characterized by a different activation energy. The first regime was observed

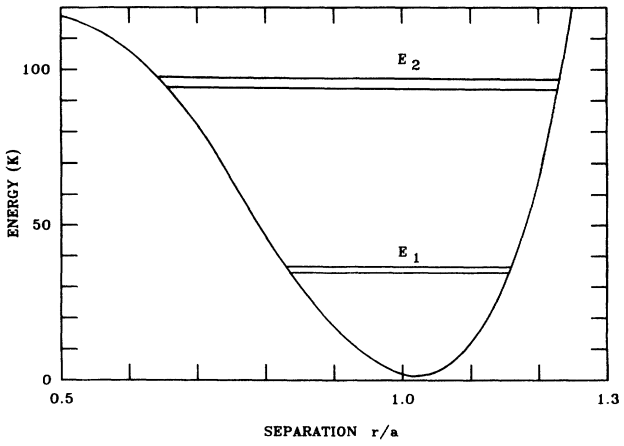

FIG. 1. Vacancy-molecule interaction potential for solid H_2 (after Ebner and Sung, Ref. 23). E_1 and E_2 are the two bound states, 34.1 K and 95.4 K, respectively; and each level is shown as a doublet, corresponding to the tunneling, $J_1 = 0.15$ K and $J_2 = 5.1$ K, respectively.

in early NMR studies of solid hydrogen,[24–28] and in this paper, we discuss the result of high-sensitivity tests for quantum tunneling in the low-temperature regimes.

In the remainder of this section, we will introduce the relevant definitions and terminology for discussing the properties of vacancies in quantum solids. In Sec. II, we review the theory of vacancy formation and propagation, and outline the theory of vacancy-induced NMR relaxation in Sec. III. The experimental arrangement is discussed in Sec. IV and the results and their analyses are presented in Sec. V. Point defects are defined as any irregularities in which the microscopic arrangement of the atoms or molecules differs drastically from the perfect crystalline lattice structure, and which are bounded on the atomic scale in three dimensions; line and surface defects are bounded in two and one dimensions, respectively.

Vacancies are present in thermal equilibrium in all crystals (at $T>0$) because of the increase in entropy resulting from the disorder caused by their presence. If there are N atoms (or molecules), and n vacant sites, minimization of the Gibb's free energy ($G=U-TS+PV$) shows that the fractional concentration of vacancies at temperature T is given by

$$X=n/N=\exp(-\Phi_F/k_BT)\ , \tag{1}$$

where Φ_F is known as the vacancy formation energy.

$$\Phi_F=\varepsilon_0+PV_0\ , \tag{2}$$

where V_0 is the atomic volume, P is the pressure, and

$$\varepsilon_0=\frac{\partial V_{eqm}}{\partial n}\ , \tag{3}$$

where ε_0 is the temperature-independent potential energy needed to remove one atom and put it on the surface of the crystal in the case of a Schottky defect, or at an interstitial site in the case of a Frenkel defect.

It is worthwhile to note that line and surface defects are very different to point defects. The cost in energy of creation of point defects is compensated by the gain in entropy ($\sim \ln n$), but this is, in general, not the case for line and surface defects. Point defects can also move more freely than line and surface defects.

Because of the presence of vacancies, atoms (or molecules) can move from one site to another in a crystal via the vacant sites. The atomic flux $\mathbf{J}$ is related to vacancy concentration gradient by Fick's first law

$$\mathbf{J}=\mathsf{D}\cdot\nabla n\ , \tag{4}$$

where the tensor D defines the diffusivity of the solid. For an isotropic solid, D reduces to a scalar, the diffusion constant D which is often observed to obey an Arrhenius behavior with

$$D=D_0\exp(-E_A/k_BT)\ , \tag{5}$$

where E_A is called the activation energy and D_0 is a prefactor. In general, we expect E_A to be the sum of the vacancy formation energy Φ_F and a potential barrier height V_B describing the potential that an atom must overcome in order to move into a neighboring vacant site. One of the most exciting discoveries in recent years in the study of quantum solids is the observation that for low-density bcc solid ^{3}He, the activation energy E_A [as seen by NMR (Refs. (15)–(18)] is equal to the formation energy Φ_F (as seen by x-rays[9–14]). This indicates that the atoms move by *quantum tunneling* through the intervening barrier.

Measurements of vacancy-induced diffusion in solids is often based on the observation of Fick's second law

$$\frac{\partial n}{\partial t}=D\nabla^2 n \tag{6}$$

obtained from the first law by use of the continuity equation. The relaxation of the vacancy density n, following a disturbance away from the equilibrium value, can then be used to determine D. NMR methods provide a particularly advantageous method of studying diffusion because (1) it is applicable to a large number of materials, and (2) it is nondestructive. As a result of the diffusion of the atoms, the nuclear magnetic interactions between the atoms become time dependent, and this can be studied in detail. Because the local magnetic fields tend to be averaged out by the rapid motion of the atoms, the NMR line shape is narrowed as a result of the diffusion and this can be measured as a function of the temperature. More precisely, the relaxation of the longitudinal component of the nuclear magnetization (i.e., that component parallel to the applied field), and the relaxation of the transverse component depend on the spectral weights of the atomic motions at different frequencies, and detailed information about the vacancies and their motions can be deduced from measurements of the longitudinal relaxation time T_1 and the transverse relaxation time T_2. This will be discussed in detail in Sec. III.

II. VACANCY FORMATION AND PROPAGATION

In order to calculate the vacancy formation energy, we need to know the ground-state function for the quantum crystal.[32,33] The first step is to calculate the energy to form the vacancy without any deformation of the crystal (i.e., neglecting the increased spread and the shift of the particle wave functions for lattice sites near the vacancy). There are two main contributions: (i) PV_0, the energy to expand the crystal by one atomic volume (V_0) at constant pressure (P), and (ii) the energy required to move an atom (from the vacant site) to the crystal surface. For a Gaussian wave function

$$\phi_j(\mathbf{r})=\left[\frac{A}{\pi}\right]^{3/4}\exp[-\tfrac{1}{2}A(\mathbf{r}-\mathbf{R}_j)^2] \tag{7}$$

for a particle at lattice site $\mathbf{R}_j$, the formation energy for an undistorted lattice is

$$\Phi_F^{\text{und}}=PV_0-E_0+\frac{3\hbar^2A}{4m}\ . \tag{8}$$

E_0 is the ground-state energy per particle, and m is the particle mass. For the distorted lattice, one only needs to consider the z nearest neighbors of the vacancy, and if we replace A by A_D for the distorted case, the formation en-

ergy becomes

$$\Phi_F^D=\Phi_F^{\text{und}}+\frac{3z}{8}\frac{\hbar^2}{m}(A_D-A)\ . \tag{9}$$

A_D is determined self-consistently by minimizing the formation energy and the crystal free energy. In addition to the effect of the lattice distortion near the vacancy, one needs to calcualte the effect of jumping, or particle-vacancy exchange on the energy values. This is particularly important in solid ^{3}He where the vacancies must be considered as delocalized because the atom-vacancy exchange frequencies are known experimentally to be of the order of 10^9-10^{10} Hz.[15-17] The vacancy tunneling can be calculated from the overlap of the atomic wave functions, and is given by

$$\omega_V=\frac{\hbar^2 A_D}{m}\left[\frac{A_D a_0^2}{\pi}\right]^{1/2}\exp(-\tfrac{1}{4}A_D a_0^2)\ , \tag{10}$$

where a_0 is the nearest-neighbor separation. The numerical values of ω_V given by this formula are of the same order of magnitude as those deduced from NMR experiments.[15] The effect of tunneling energies is very important for solid He^3 because they are a significant fraction of the formation energy Φ_F. The vacancies in ^{3}He are therefore regarded as delocalized and forming an energy band with width $\Delta E\simeq z\omega_v$. The vacancies in the solid heliums are therefore believed to travel coherently as vacancy waves at low temperatures rather than hopping randomly as classical point defects. Because of the stronger binding energies in solid H_2, the delocalization of the vacancies is expected to be much less significant and not to affect the formation energy appreciably, but detailed measurements of the microscopic dynamics as seen by NMR experiments are expected to show tunneling effects.

Ebner and Sung[23] have calculated the ground-state energy of a vacancy in solid H_2 using the self-consistent method described above. What is particularly interesting for H_2 is that there are two bound states for the particle-vacancy interaction potential at $E_1=34.1$ K and $E_2=95.4$ K (at $P=0$). The energy barrier to classical particle-vacancy exchange (the barrier height of Fig. 1) is $V_B=85$ K as measured from the level E_1 to the top of the barrier. Ebner and Sung have also calculated the tunneling energies for both states and find $J_1=3.1\times10^9$ Hz (0.150 K) and $J_2=1.1\times$and10^{11} Hz (5.14 K).

Using Fermi's golden rule, one can calculate the transition probability for a vacancy tunneling from lattice site $\mathbf{R}_j$ to site $\mathbf{R}_l$ where the local crystal fields (for particle displacement) are Δ_j and Δ_l, respectively. The rate per unit time is

$$W_{jl}=2\pi\omega_V^2\delta(\Delta_j-\Delta_l)\ . \tag{11}$$

The diffusion constant for the vacancy motion can be calculated assuming the random-walk formula

$$D=\tfrac{1}{6}\sum_j R_{jl}^2 W_{jl}\ , \tag{12a}$$

$$=\tfrac{1}{6}a_0^2 f X_V\sum_n W_n P_n\ , \tag{12b}$$

where a_0 is the nearest-neighbor lattice spacing, f is a correlation factor (of order unity) which specifies the extent to which the jumps are not random,

$$X_V=\exp[-(F_v/k_BT)]$$

is the vacancy concentration or probability that a given site is vacant (F_v being the vacancy free energy), W_n is the jumping rate from energy level n (=1 or 2) of Fig. 1, and P_n is the probability that level n is occupied. For quantum-mechanical tunneling through the energy barrier $W_n=J_n/\pi$ (assuming $\Delta_j=\Delta_e$), and for classical thermal activation over the energy barrier V_B,

$$W_{\text{therm}}=(V_B/m_0^2)^{1/2}\ .$$

The self-diffusion rate for vacancy-particle motion, considering all processes, is

$$D=\tfrac{1}{6}a_0^2\left[\sum_n(J_n/\pi)P_n+(V_b/ma_0^2)^{1/2}e^{-V_B/k_BT}\right]\times e^{-\Phi_F/k_BT}\ . \tag{13}$$

Using the values calculated by Ebner and Sung[23] this yields

$$D=2\times10^{-6}(1+34e^{-61/T}+300e^{-85/T})\times e^{-112/T}\ \text{cm}^2/\text{sec}\ . \tag{14}$$

This theoretical expression for the self-diffusion constant is unusual in that there are two well-defined temperature ranges: (i) classical thermal activation at high temperatures with an activation energy $E_A=\Phi_F+V_B=197$K for

$$T>(E_B-E_2)/\ln(W_{\text{class}}/J_2)\simeq 11\ \text{K}\ ,$$

and (ii) quantum-mechanical tunneling at low temperatures with $E_A=\Phi_F=112$ K for $T<11$ K. It is important to note that although there are three terms in the expression for D [Eq. (14)] with different temperature dependence, there are only two temperature regimes because the second term in Eq. (14) does not dominate for any temperature. The first term dominates the second term for

$$T<(E_2-E_1)/\ln(J_2-J_1)\simeq 17\ \text{K}$$

(corresponding to $E_A=\Phi_F+E_2-E_1\simeq 173$ K). One therefore expects to observe only regime (i) with $E_A=197$ K from melting (14 K) to approximately 11 K followed by quantum tunneling with $E_A=112$ K.

The self-diffusion constants can be determined from measurement of the nuclear spin-lattice relaxation time T_1, and this is discussed in the next section.

III. NUCLEAR MAGNETIC RELAXATION

NMR is sensitive to the presence of vacancies through their diffusive motion As the vacancies migrate through the lattice by exchange with atoms or molecules, the intermolecular nuclear spin-spin interactions become time dependent because of the molecular motion. The spectral components of the motion at the nuclear Larmor fre-

quency ω_L and $2\omega_L$ (see below) determine the nuclear-spin-lattice relaxation induced by the vacancy motion.

The relation between the microscopic vacancy tunneling frequency ω_V calculated in Sec. II and the characteristic frequencies that determine the modulation of the nuclear spin-spin interactions need to be established with care.[6,34] If in a given crystalline structure, a vacancy can migrate from a given lattice site to a neighboring site with a characteristic frequency ω_{m0}, the time-dependent jump frequency for a given molecule is

$$\omega_m(T)=X_V(T)\omega_{m0} , \tag{15}$$

where $X_V(T)$ is the number of vacancies in thermal equilibrium at temperature T. ω_{m0} is related simply to the tunneling frequency ω_V by a numerical constant which depends on the lattice structure. Moment calculations[6] show that for tunneling involving only nearest neighbors

$$\omega_{m0}=A\omega_V , \tag{16}$$

with $A=Z\sqrt{2\pi/15}$ for coordination number Z. The intermolecular dipole-dipole interaction between *two* molecules are modulated at a rate

$$\omega_D=2\omega_m$$
$$=2AX_V(T)\omega_V . \tag{17}$$

NMR experiments can therefore be used to determine the microscopic jump frequency ω_V, and the formation energy and barrier energies through the absolute values and the temperature dependence of the relaxation times, respectively. The nuclear magnetic relaxation can be described in terms of an energy bath model consisting of several energy reservoirs: the nuclear Zeeman energy (Z), the vacancies (V), the tunneling excitations (E), the phonons (P), and the thermal bath (or walls) (B). If the Zeeman energy is perturbed, thermal equilibrium is restored by transitions between the nuclear Zeeman energy levels induced by the fluctuations of the dipole-dipole interactions. If the dipolar interactions are expressed in terms of irreducible tensorial operators T_{lm} (which transform analogously to the spherical harmonics Y_{lm}), the relaxation rate (for a polycrystalline sample) is given by

$$\frac{1}{T_1}=\tfrac{2}{3}M_2\sum_{m=1,2}m^2\mathcal{J}_{lm}(m\omega_L) , \tag{18}$$

where M_2 is the Van Vleck second moment for the dipole-dipole interactions, and the $\mathcal{J}_{lm}(m\omega_L)$ are the spectral densities of the spin-spin correlation functions $\langle T_{lm}(t)T_{lm}^{\dagger}(0)\rangle$ at the nuclear Larmor frequency ω_L.

The $\mathcal{J}_{lm}(m\omega_L)$ are difficult to evaluate directly from the microscopic motion and are often approximated by Lorentzian functions.

$$\mathcal{J}_{21}(\omega_L)=\omega_D^{-1}/[1+(\omega_L/\omega_D)^2] . \tag{19}$$

At very low temperatures, the number of vacancies is too small to provide an effective interaction, and this vacancy-induced relaxation mechanism becomes "frozen out" and other processes take over. In solid ^{3}He, particle-particle exchange will also modulate the dipolar interactions and provide a low-temperature relaxation mechanism which will be effective for $\omega_L \lesssim J_3$ (the exchange frequency). When this mechanism is inefficient (at high magnetic fields) relaxation is believed to occur by phonon modulation[16] of the spin interactions or by nuclear spin diffusion.[35]

In solid H_2 we must consider the two distinct molecular species corresponding to the two independent ways of satisfying the Pauli exclusion principle. The ortho species has a symmetric nuclear wave function χ_n ($I_{\text{total}}=1$) and odd orbital angular momentum ($J=1$ need only be considered at low temperatures). The para species with antisymmetrical χ_N ($I_{\text{total}}=0$) and even orbital wave function ($J=0$ at low temperatures) is not observed by NMR.

In addition to the relaxation mechanisms discussed above, there is a competing mechanism for the relaxation of ortho-H_2 resulting from the modulation of the intramolecular dipole-dipole interaction of each molecule by rapid molecular reorientations. The latter is determined by the electric quadrupole-quadrupole (EQQ) interactions between ortho molecules, and it overwhelms the vacancy-induced mechanism except for temperatures close to the melting point where the number of vacancies is high. Weinhaus and Meyer[27] observed vacancy-induced relaxation for $10.5\ \text{K} < T < 13.5\ \text{K}$ for relatively high ortho concentrations and observed a variation in T_1 by a factor of 5. Bloom[24] saw only the EQQ mechanism for solid H_2, but did observe vacancy effects for solid HD.

In order to test for the possible quantum tunneling of vacancies in solid H_2, we needed to observe vacancy relaxation at temperatures significantly lower than those previously studied. We therefore chose to study samples containing low ortho-H_2 concentrations (0.5–2.5 %) and prepared with small concentrations of HD impurities (typically 1%). (The natural HD abundance is 0.04%). The ortho-H_2 molecules relax very rapidly via the EQQ mechanism with

$$T_{1Q}=1.76(\Gamma/k_B)X^{5/3}$$

for these ortho concentrations and at high temperatures.[36] The direct relaxation of the HD molecules to the lattice is, however, very slow and one observes an indirect

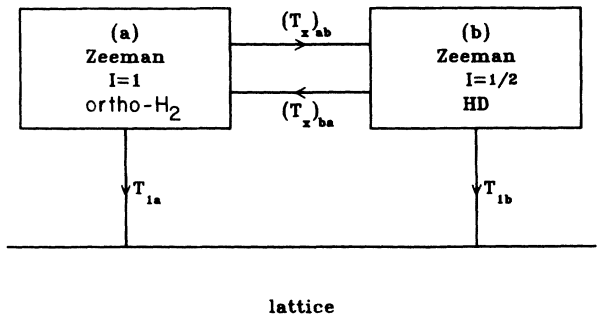

FIG. 2. Schematic representation of the coupling and relaxation of the two nuclear spin energy baths for (a) ortho-H_2, and (b) HD molecules.

relaxation mediated by the spin-spin coupling between the HD molecules and the ortho-H_2 molecules.

The cross relaxation can be analyzed by treating the ortho-H_2 spins and the proton spins of the HD molecules as two weakly coupled energy reservoirs, a and b, respectively (see Fig. 2).[24] The coupled rate equations for the inverse nuclear spin temperatures, λ^a and λ^b of the two energy baths, is given by[24,27]

$$\frac{d\lambda^a}{dt}+\left[\frac{1}{T_1^{aa}}+\frac{1}{(T_x^{ab})_1}+\frac{1}{(T_x^{ab})_2}+\frac{1}{T_x^{ab})_0}\right](\lambda^a-\delta^a)=\left[\frac{1}{(T_x^{ab})_0}-\frac{1}{(T_x^{ab})_2}\right](\lambda^b-\delta^b)\ , \tag{20a}$$

$$\frac{d\lambda^b}{dt}+\left[\frac{1}{T_1^{bb}}+\frac{1}{(T_x^{ba})_1}+\frac{1}{(T_x^{ba})_2}+\frac{1}{(T_x^{ba})_0}\right](\lambda^b-\delta^b)=\left[\frac{1}{(T_x^{ba})_0}-\frac{1}{(T_x^{ba})_2}\right](\lambda^a-\delta^a)\ . \tag{20b}$$

$\lambda^{a(b)}=\gamma_{a(b)}\hbar B/k_B T_s^{a(b)}$ and $\delta^{a(b)}=\gamma_{a(b)}\hbar B/k_B T_L$, where $\gamma_{a(b)}$ are the nuclear gyromagnetic ratios, B is the applied magnetic field, and $T_s^{a(b)}$ and T_L are the nuclear spin temperatures and lattice temperature, respectively. T_1^{aa} and T_1^{bb} are the relaxation times in the absence of any coupling. The $(T_x^{ab})_m$ represent the cross-relaxation processes given by

$$\frac{1}{(T_x^{ab})_1}=\tfrac{2}{3}M_2^{ab}(X)\mathcal{J}_{21}^{ab}(\omega_a)\ , \tag{21a}$$

$$\frac{1}{(T_x^{ab})_2}=\tfrac{4}{3}M_2^{ab}(X)\mathcal{J}_{22}^{ab}(\omega_a+\omega_b)\ , \tag{21b}$$

$$\frac{1}{(T_x^{ab})_0}=\tfrac{2}{9}M_2^{ab}(X)\mathcal{J}_{20}^{ab}(\omega_a-\omega_b)\ , \tag{21c}$$

$$\frac{1}{T_x^{ba}}=f\frac{1}{T_x^{ab}},\quad f=\frac{N_a I_a(I_a+1)}{N_b I_b(I_b+1)}\ . \tag{21d}$$

N_a and N_b are the number densities for the a and b spins, respectively. $M_2^{ab}(X)$ is the rigid lattice second moment for the intermolecular dipole-dipole interactions between the a and b spins for an ortho concentration X. The J_{lm}^{ab} are the spectral densities for the (lm)th component of the dipolar interactions, and ω_a and ω_b are the nuclear Larmor frequencies of the a and b spins, respectively.

The interest in studying the cross-relaxation process is that for a coupling between nonidentical nuclei, the flip-flop terms of type $I_a^+ I_b^-$ in the dipole-dipole coupling between the different spins are effective in the relaxation and lead to a contribution which depends on the spectral density

$$\mathcal{J}_{20}(\omega_a-\omega_b)=\mathcal{J}_{20}(0)\ .$$

This contribution at zero frequency is especially useful for studying vacancy motion at low temperatures. Because of the small number of vacancies at low temperatures, the characteristic frequency of vacancy motion

$$\omega_m=X_V(T)\omega_{m0}\ll\omega_a,\omega_b$$

and the term $\mathcal{J}_{20}(0)\approx\omega_D^{-1}(T)$ dominates the relaxation rate. In order to ensure that this is true throughout the full temperature range up to the melting point, we carried out experiments in high magnetic fields ($\omega_L=268$ MHz). In the temperature range of interest $X_V(T)\lesssim 10^{-4}$ and $\omega_D(T)\ll\omega_L$, $\mathcal{J}_{20}(0)\gg\mathcal{J}_{21}(\omega_L)$ and

$$\mathcal{J}_{22}(2\omega_L)\approx\omega_D^{-1}/[1+(2\omega_L/\omega_D)^2]\ .$$

The analysis of the relaxation is particularly straightforward in this case and this is especially important in order to be able to test for the different temperature dependences of the two types of vacancy propagation.

The ortho-H_2 molecules relax rapidly to the lattice via the EQQ mechanism, $T_{1,Q}\approx 2$–4 msec for $X(\text{ortho})\simeq 0.5$–$2\,\%$, and one observes the cross relaxation of the HD molecules (the b spins) to the ortho-H_2 molecules (the a spins). The cross-relaxation rate is given by

$$\frac{1}{(T_x^{ba})}=\tfrac{2}{9}fM_2^{ab}(X)\mathcal{J}_{20}(0)\ , \tag{22}$$

with $\mathcal{J}_{20}(0)=\omega_D^{-1}(T)$. ω_D is the modulation frequency of the HD-ortho H_2 dipole-dipole interaction. At high temperatures where the motion of molecules, either HD or ortho-H_2 molecules, into vacant sites determines the modulation frequency, $\omega_D=2\omega_m$ as in Eq. (17). At low temperatures, however, only the HD molecules are believed to be mobile because of particle-particle exchanges. Any possible exchange of ortho-H_2 molecules is "quenched" because of the relatively strong anisotropic interaction between ortho molecules due to their electric quadrupole-quadrupole (EQQ) interactions. The tunneling energies ($\sim 10^{-6}$ K) are much smaller than the EQQ energies (~ 1 K), and only the very small fraction of tunneling processes that conserve total energy are allowed. The tunneling of ortho-H_2 molecules would therefore be much smaller than para-H_2 or HD molecules. In this latter case the dipolar modulation frequency $\omega_D=\omega_T$ (HD), the HD tunneling frequency.

Studies of the HD-ortho H_2 cross relaxation allow one to explore the temperature dependence of the vacancy motion over a wider temperature range than possible in previous studies.[24–28] This is possible because the relatively fast quadrupolar relaxation is in "series" with the cross relaxation, and does not mask the vacancy-induced relaxation as it does if one studies the nuclear spin-lattice relaxation of ortho-H_2 molecules alone. Determination of the characteristic motional frequencies $\omega_D(T)$ from the NMR studies also allows one to calculate the self-diffusion constant from the relation $D=\frac{1}{6}a_0^2\omega_m(T)$.

IV. EXPERIMENTAL METHOD

The nuclear-spin-lattice relaxation-time measurements were carried out using a phase-coherent pulse system operating at 268 MHz. $(\pi/2)-\tau-(\pi/2)$ rf pulse sequences were used to determine T_1. Narrow (8–10 μsec) high-power rf pulses were used to cover the complete NMR spectrum of both the HD impurity molecules and the ortho-H_2 molecules. The amplitude of the rf magnetic field in the rotating frame was 12 G. Washburn *et al.*[38] used very long rf pulses (100–150 μsec) in order to saturate only the relatively narrow HD component of the spectrum, but the interpretation of the relaxation is difficult for the long, low-power pulses[39] and we therefore worked in the short-pulse limit.

In order to prepare samples with the desired ortho-H_2 and HD concentrations, we initially prepared gas samples at room temperature containing 1.1% HD and "normal" H_2 (75% ortho-H_2). The mixture was then condensed into an ortho-para converter cell containing chromic oxide gel as a catalytic converter and which was located a short distance from the NMR cell. The required ortho concentration was obtained by regulating the temperature of the converter very accurately and allowing the ortho-H_2 to convert to the thermal equilibrium value. The converted mixture was then transferred to the NMR cell by lowering the temperature of the cell. After condensation in the NMR cell, the samples were carefully annealed at 13.5 K. The final ortho concentration was determined unambiguously by direct comparison of the very distinct NMR echo shapes of the HD and ortho-H_2 contributions at temperatures below 1 K (see Fig. 3). This method of determining the ortho concentration was used to check the reliability of the conversion process by monitoring the concentration measured by the NMR method as a function of the converter temperature T_0. As shown in Fig. 4, the concentration was very accurately determined by the holding temperature T_0 for concentrations $0.002 < X < 0.03$.

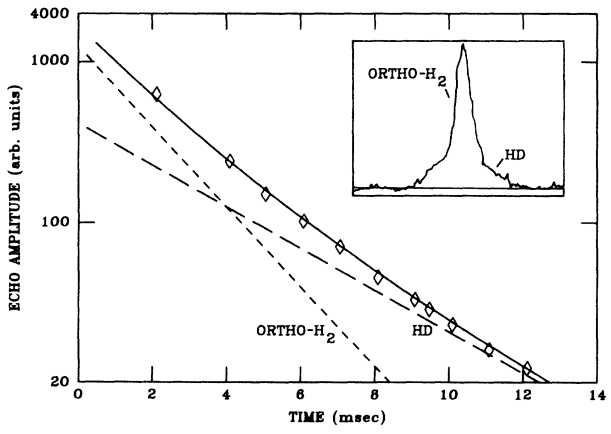

FIG. 3. Typical relaxation of the NMR echoes (for a $\pi/2-\tau-\pi/2$ sequence) as a function of time at low temperatures ($T=0.22$ K). The two slopes are attributed to the HD (1.1%) and ortho-H_2 (1.6%) molecules. The inset illustrates the distinct HD and ortho-H_2 components of the echoes at low temperatures.

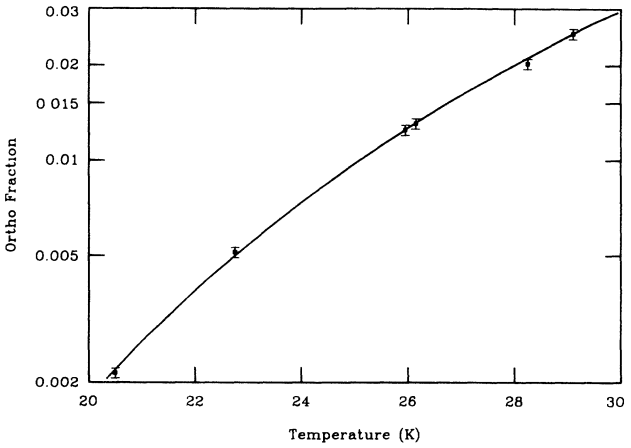

FIG. 4. Comparison of the ortho-H_2 concentrations obtained from the *in situ* orthopara converter at temperature T with the equilibrium value calculated for free molecules (solid curve). The ortho-H_2 concentrations were determined from comparisons of the HD and ortho-H_2 echo amplitudes at low temperatures (see Fig. 3).

The NMR cell consisted of a Kel-F sample chamber (3 mm i.d., 3 mm length) (see Fig. 5). Both ends of the cell were sealed by cylindrical copper end caps which were carefully machined to a diameter slightly larger than that

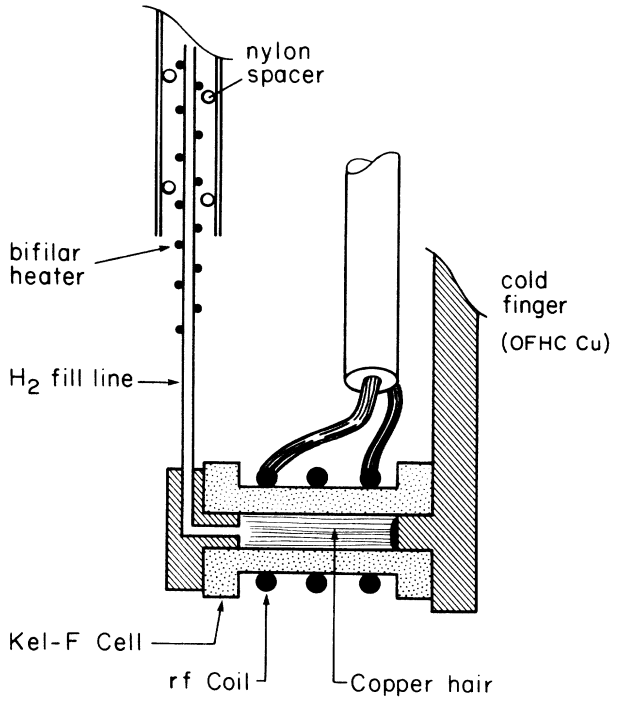

FIG. 5. Schematic drawing of the NMR cell. The coil former is machined from Kel-F and forms a heat-shrink fit over the copper end caps.

of the Kel-F chamber, and a seal reliable to 150 bars was obtained by the thermal contraction of the Kel-F following initial warming to 150°C during assembly. One of the end caps formed an integral part of a thermally regulated cold finger of oxygen-free high-conductance (OFHC) copper while the other was fed by the hydrogen fill line. Thermal contact to the sample was ensured by a brush of very fine copper wires (0.001 mm o.d.) soft soldered to the cold finger.

The temperature was monitored by a calibrated carbon-glass thermometer[40] attached to the copper cold finger of the NMR cell. The temperatures were also checked using the total NMR absorption signal as a measure of the mean temperature of the hydrogen sample. The NMR method was unreliable near the melting point because a portion of the sample tended to migrate up the fill line, and we relied on the carbon glass thermometer to determine the temperature in this region. The radio frequency coil wound around the sample chamber was connected to an rf-pulse duplexer (at room temperature) by a homemade cryogenic cable (stainless steel outer conductor, brass inner conductor, Teflon dielectric, and nominally 50 Ω) cut to $3\lambda/2$. The duplexer was a "lumped-circuit" designed to optimize the matching of the rf power pulse to the NMR circuit while protecting the receiver. The output of the duplexer was amplified by a three-stage, low-noise, narrow-band ultrahigh-frequency (ufh) amplifier employing dual-channel metal-oxide-semiconductor field-effect transistor (MOSFET) transistors.[41] The output of the amplifier was detected coherently using a doubly balanced mixer where the local oscillator source was derived from the rf generator which fed the gates of the rf pulse system. An adjustable coaxial line was used to obtain the correct phase of the source at the mixer. After coherent detection, automated signal averaging techniques were used to record the free-induction decays following each pulse.

V. EXPERIMENTAL RESULTS AND DISCUSSION

The nuclear spin-lattice relaxation times T_1 were determined by monitoring the recovery of the free-induction decay following the second pulse of the $(\pi/2)-\tau-(\pi/2)$ sequence as a function of τ. The repetition of the pulse sequence was kept to longer than $20T_1$ to ensure full recovery of the magnetization between pulse sequences.

The relaxation was observed to consist of two contributions: (i) a fast relaxation over a short time (~ msec) which we attribute to the ortho-H_2 relaxation via the EQQ mechanism (see Fig. 6), and (ii) a long time component which we interpret as the cross-coupling relaxation T_x between the HD molecules and ortho-H_2 molecules. The relative amplitudes of the two components were consistent with the known concentrations of the HD and ortho-H_2 molecules.

While the short time relaxation exhibited little temperature dependence, the long time component showed a very strong dependence consistent with that expected for vacancy-induced relaxation. The temperature dependence observed for the long time relaxation is shown in Fig. 7. Three distinct temperature regimes are observed: (1) at low temperatures $T<7$ K, T_x has only a weak approximately linear temperature dependence; (2) at intermediate temperatures 7 K $< T <$ 11 K, T_x passes through a minimum, and (3) above 11 K, T_x increases exponentially with temperature until the sample melts. These results are similar to those observed for the transverse nuclear spin relaxation T_2 in similar shapes,[29] but with the important difference that the variation of T_x as a function of temperature is much more dramatic than that observed for T_2. T_x varies by a factor of 6000 in the high-

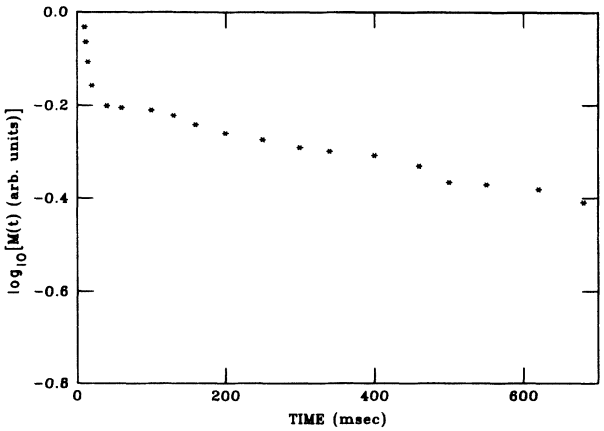

FIG. 6. Typical relaxation of magnetization showing the very short time component attributed to the direct nuclear spin relaxation of ortho-H_2 molecules to the lattice. $M(t)$ is the magnetization determined from the free induction decay at $T=11.5$ K.

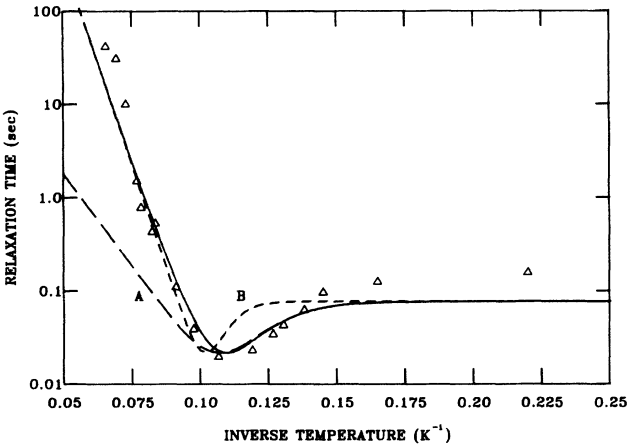

FIG. 7. Temperature dependence of the observed nuclear spin-lattice relaxation of HD impurities (1.1%) in solid H_2 (1.8% ortho). The solid line is calculated for a vacancy-induced relaxation if vacancy quantum tunneling is included, and the broken lines describe the contribution for classical diffusion alone for an activation energy (a) of 91 K and (b) of 198 K. The observed relaxation is attributed to cross relaxation between the HD impurities and the ortho-H_2 molecules.

temperature regime (T_2 varies by approximately 100), and near the minimum T_x varies by a factor of 12 (T_2 by 1.6).

The mechanism for cross relaxation in the high-temperature regime ($T > 11$ K) is attributed to the motion of vacancies (with characteristic exponential temperature dependence), and at very low temperatures the relaxation is believed to be associated with particle-particle exchange (e.g., exchange of HD and para-H_2 molecules on neighboring sites). The distinct minimum observed for T_x at intermediate temperatures was not predicted, but a similar but much shallower minimum was observed for the spin-spin relaxation time T_2 in earlier studies.[29] We believe that the minimum is due to the same effect in both cases. Because of their tunneling the HD molecules can be regarded as delocalized and their propagation can be described as wavelike excitations as described by Andreev and Lifshitz[4] for quantum crystals in general. In this case, as one warms from very low temperatures, the initial effect of the introduction of vacancies will be to provide additional scattering centers for the impurity motion which will decrease the effective modulation frequency of the dipolar interactions and thus reduce the relaxation time. Eventually as one warms further, the vacancy motion becomes much more effective than the impurity motion, and the relaxation time increases because of the increase in the effective modulation frequency ω_D with the number of vacancies.

The analysis of the temperature dependence observed for T_x required three steps: (1) determining the HD motional frequency to fit the low-temperature behavior, (2) determining the vacancy formation energy, barrier energy, and frequencies of tunneling motion and classical activation energy to fit the high-temperature behavior, and (3) estimating the vacancy-impurity scattering cross section to describe the intermediate-temperature regime. For the analysis of the T_x data, we used the values of the particle-particle exchange frequency deduced from the T_2 studies, and the vacancy scattering model of Locke[42] was used to describe the minimum. The number of adjustable parameters is thus reduced to only those describing the vacancy diffusion in Eqs. (13) and (16), namely the activation energy, the barrier height, the classical jump rate, and the quantum tunneling rate. We will now discuss the results of the analysis for each temperature regime.

A. The high-temperature regime

The temperature dependence observed at high temperatures cannot be described in terms of a single thermal activation energy for the vacancy motion. We therefore included a quantum tunneling term analogous to that proposed by Ebner and Sung[23] in order to obtain an accurate quantitative fit. The best fit (solid line of Fig. 7) as obtained using Eq. (22) for the relaxation rate with a characteristic dipolar modulation frequency

$$\omega_D = 2Z\sqrt{2\pi/15}X_V(T)\omega_V$$
$$= 4.4\times10^9 e^{-91/T}(1+5.1\times10^4 e^{-107/T}) . \quad (23)$$

Note that following the discussion in Sec. II we do not include the intermediate term of Ebner and Sung [the second term in Eq. (14)] as this is believed to be dominated by the other terms for all temperatures.

At high temperatures the activation energy was observed to be 198±6 K in agreement with earlier studies.[24–28] The prefactor of the classical diffusion constant $D = D_0 e^{-E_A/T}$ can be determined from the prefactor of Eq. (23) and using the relation $D = \frac{1}{6}a_0^2\omega_m(T)$. From our results we found

$$D_0^{\text{class}} = (4.9\pm1.1)\times10^{-3}\text{cm}^2\text{sec}^{-1} ,$$

which is also in good agreement with previous determinations (see Table I). For the overall fit described by Eq. (23), $\Phi_F = 91$ K is the vacancy formation energy and $V_B = 107$ K is the potential barrier height. The values of T_1 calculated for a single activation energy alone (classical diffusion) is shown by the broken lines of Fig. 7: (a) for an activation energy of 91 K which best describes the behavior on the low-temperature side of the minimum (see the discussion below), and (b) for an activation energy of 198 K which provides the best fit at very high temperatures.

B. The intermediate-temperature range

The fit shown by the solid line in Fig. 7 for the full temperature range, and in particular for the observed minimum, depends on the inclusion of the particle-particle tunneling, and we used the same model as that proposed to describe the temperature dependence of the

TABLE I. Values of the parameters in the diffusion constant $D = (D_0^{qu} + D_0^{\text{class}} e^{-V_B/T}) e^{-\Phi_F/T}$.

Reference	Φ (K)	V_B (K)	$\Phi_F + V_B$ (K)	D_0^{qu} (10^{-8} cm^2/sec)	D_0^{class} (10^{-3} cm^2/sec)
This study	91±6	107±3	198±6	9.8	4.9
Zhou *et al.* (Ref. 29)	91±10	104±5	195±10	1.9	5.1
Bloom (Ref. 24)			191		
Hass *et al* (Ref. 26)			198		3.8
Weinhaus *et al* (Ref. 27)			200±10		3.0
Ebner and Sung (Ref. 23)	112	85	197	200	0.6

nuclear spin relaxation of ^{3}He impurities in solid ^{4}He.[4,5,43,44] The low-temperature relaxation is attributed to particle-particle quantum exchange of the HD impurity molecules with the host lattice molecules (para-H_2). Recent T_2 studies[31] of HD molecules in solid H_2 have also been interpreted in terms of impurity-particle exchange. In this model the HD particles travel through the lattice in the same manner as the vacancies, but with much smaller exchange frequencies. The relaxation occurs via the modulation of the magnetic interaction between the HD molecules and the ortho-H_2 molecules when the former are scattered by the elastic deformation field around the effectively static ortho-H_2 molecules. The cross-relaxation rate is given by

$$\frac{1}{T_x^{ab}} = \tfrac{2}{9} M_2^{ab}(X)/J_{\text{eff}} , \tag{24}$$

where the effective exchange frequency J_{eff} for the relaxation is related to the microscopic exchange rate J by[45] $J_{\text{eff}} = J_x(U_0/J)^{2/n}$ for a scattering interaction potential $U(R) = U_0(a_0/R)^{2/n}$. The results of the T_2 studies,[29] $J_{\text{eff}}/2\pi = 9.7\times10^4$ Hz and $J/2\pi = 9.4\times10^3$ Hz, were used in the analysis of the low-temperature behavior shown in Fig. 7.

As a result of their tunneling the HD impurities are believed to be delocalized and propagate as wavelike excitations at low temperatures. The minimum in T_1 occurs because on warming above 7 K the coherent motion of the impurities is interrupted by scattering by vacancies rather than by the ortho-H_2 impurities. The temperature at which this crossover occurs can be estimated from the condition that the effective scattering by vacancies becomes comparable to that by ortho-H_2 molecules. This occurs when $X_V(T)\omega_V \gtrsim X(\text{ortho-H}_2)J$, i.e., for $T > 6.6$ K, which is in good agreement with the experimental results.

When the vacancy scattering mechanism becomes effective, J_{eff}^{-1} must be replaced by[42]

$$J_{\text{scatt}}^{-1}(T) = J_{\text{eff}}^{-1} + \omega_{\text{IV}}^{-1}(T) , \tag{25}$$

where

$$\omega_{\text{IV}} = \frac{2\pi}{3} J^2/X_V(T)\omega_V(T)$$

is the impurity-vacancy scattering rate.[43] The overall temperature dependence for *both* the vacancy motion and the impurity motion is given by

$$\frac{1}{T_x^{ba}} = \frac{2f}{9} M_2^{ab}(X)\mathcal{J}_{20}(0) , \tag{26}$$

with

$$\mathcal{J}_{20}^{-1}(0) = A\,[X_V(T)\omega_V(T) + J_{\text{scatt}}(T)] .$$

$M_2^{ab}(x) = 1.24(\text{kHz})^2$ is the rigid lattice second moment for the intermolecular dipole-dipole interactions between the HD and ortho-H_2 molecules, and from Eq. (21d) $f = 6.1$. $A = 7.77$ from Eq. (16). The fit over the full temperature range given by the solid line of Fig. 6 was obtained using this spectral density and the modulation frequency of Eq. (23). The use of only a single activation energy does not describe the temperature dependence over the full range (see Fig. 7). The fit on the low-temperature side of the minimum requires a much lower activation energy than that deduced from the high-temperature behavior. This is clearly seen in the comparison of the calculations for single activation energies shown by the broken lines in Fig. 7: (a) for an activation energy of 91 K which gives the best description on the low-temperature side of the minimum, and (b) for an activation energy of 198 K which gives the best fit near the melting point. Attempts to describe the minimum in terms of a model invoking phonon-impurity scattering which would lead to a T^9 dependence (on the low-temperature side of the minimum) failed to provide even a qualitative fit. We conclude that both the quantum tunneling term and the classical activation term in Eq. (23) are needed to fully describe the propagation of vacancies in solid hydrogen.

C. The low-temperature regime

As discussed above, a complete fit of the data, especially in the vicinity of the minimum, requires the introduction of a particle-particle exchange frequency to describe the motion of the HD molecules. The fit at low temperatures is therefore a test of self-consistency of the model of the cross relaxation and the interpretation of independent studies[29] of the transverse relaxation time T_2. The use of the value of the exchange frequency ($J/2\pi$) determined from the T_2 studies to describe the low-temperature regime gives a qualitatively good fit except at low temperatures, where we observe an approximately linear increase in T_x as a function of T^{-1} from 6 K to 1 K. In this temperature range the ortho-H_2 line width increases because of the slowing down of the reorientations of the ortho-H_2 molecules, and the line width of the orth-H_2 NMR spectrum increases appreciably and becomes broader than the effective motional frequency. This occurs because at low temperatures the ortho-molecules form pairs whose NMR spectrum covers 43 KHz, which is much greater

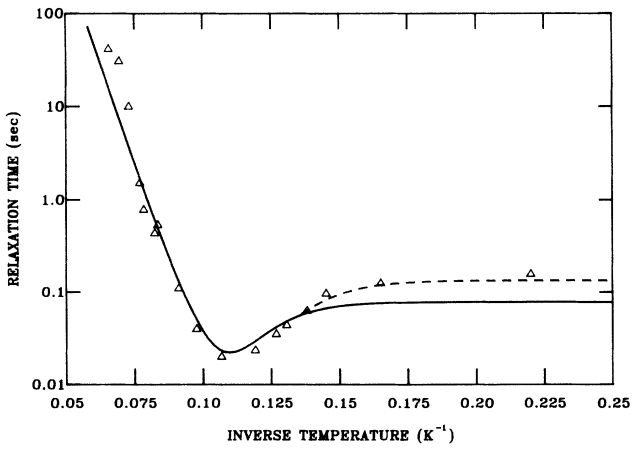

FIG. 8. Correction of calculated temperature dependence of relaxation at low temperatures to account for the broadening of the ortho-H_2 line shape relative to the HD line shape.

than that of the isolated ortho molecules. This in turn reduces the cross-relaxation rate because the "flip-flop" terms $I_a^+ I_b^-$ in the intermolecular interaction do not conserve energy. The net effect can be estimated by determining the overlap factor for the two spin species in the formulation of the two-bath relaxation scheme. In the calculation of T_x in Eq. (26), M_2^{ab} is simply scaled by a factor equal to the fraction of the ortho-H_2 spectrum which overlaps the HD spectrum. This is the method developed by Weinhaus *et al.*[27] for solid D_2 and we obtained an improved agreement for the low-temperature behavior as shown in Fig. 8.

It is important to note that the relatively long value of ~ 0.1 sec observed for the cross-relaxation time T_x at low temperatures is strong evidence for the existence of direct particle-particle exchange diffusion at low temperatures. Even for the dilute systems studied here, this is much longer than the values expected for a rigid lattice.

VI. CONCLUSION

Systematic studies of the temperature dependence of the nuclear spin-lattice relaxation of HD impurities (determined by cross relaxation to ortho-H_2 impurities) in solid H_2 have shown that the vacancy-induced relaxation observed for $7\ \text{K} < T < 13.5\ \text{K}$ cannot be described by a single activation energy. The experimental results can be understood over this temperature range if one includes a quantum tunneling contribution for the vacancy motion in addition to classical activation. Interference between vacancy motions and particle-particle tunneling (which destroys the coherence of the particle tunneling) leads to the existence of a minimum for the relaxation time at $T \simeq 9$ K with a different temperature dependence on the two sides of the minimum. On the high-temperature side of the minimum, the slope of the temperature dependence is significantly greater than that observed on the low-temperature side of the minimum. This behavior is attributed to the dominance of quantum tunneling of vacancies at temperatures $T < 11$ K. The dependence at high temperatures is in excellent agreement with that measured in previous studies.

ACKNOWLEDGMENTS

We gratefully acknowledge many helpful discussions with Mark Conradi, Jim Gaines, Erika Kisvarsanyi, Pradeep Kumar, and Horst Meyer. The research was supported by the National Science Foundation, Low Temperature Physics, Grant No. DMR-8913999, and in part by NATO Grant No. 86/703.

*Permanent address: Centre de Recherches sur les Trés Basses Temperatures, Grenoble, France.

[1]F. Seitz, in *Imperfections in Nearly Perfect Crystals,* edited by E. Shockley (Wiley, New York, 1952).
[2]C. P. Flynn, in *Point Defects and Diffusion* (Clarendon, Oxford, 1972).
[3]A. W. Chadwick and H. R. Glyde, in *Rare Gas Solids,* edited by M. L. Klein and J. A. Venables (Academic, New York, 1972), Vol. II, p. 1151.
[4]A. F. Andreev and I. M. Lifshitz, Zh. Eksp. Teor. Fiz. **56**, 2057 (1969) [Sov. Phys.—JETP **29**, 1107 (1969)].
[5]R. A. Guyer, J. Low Temp. Phys. **8**, 427 (1972).
[6]A. Landesman, Ann. Phys. (N.Y.) **9**, 69 (1975); J. Low Temp. Phys. **17**, 365 (1974); **30**, 117 (1978).
[7]J. H. Hetherington, Phys. Rev. **176**, 231 (1968).
[8]J. H. Hetherington, J. Low Temp. Phys. **32**, 173 (1978).
[9]S. M. Heald, D. R. Baer, and R. O. Simmons, Phys. Rev. B **30**, 2531 (1984).
[10]R. Balzer and R. O. Simmons, in *Low Temperature Physics LT13,* edited by D. K. Timmerhous, W. J. O'Sullivan, and E. F. Hammel (Plenum, New York, 1974), Vol. 2, p. 115.
[11]S. M. Heald, D. R. Baer, and R. O. Simmons, Phys. Rev. B **30**, 2531 (1984).
[12]P. R. Granfors, B. A. Fraass, and R. O. Simmons, J. Low Temp. Phys. **67**, 353 (1987).
[13]B. A. Fraass and R. O. Simmons, Phys. Rev. B **37**, 5058 (1988).
[14]B. A. Fraass, P. R. Granfors, and R. O. Simmons, Phys. Rev. B **39**, 124 (1989).
[15]N. S. Sullivan, G. Deville, and A. Landesman, Phys. Rev. B **11**, 1858 (1975).
[16]M. E. R. Bernier and G. Guerrier, Physica **121B**, 202 (1983).
[17]M. Chapellier, M. Bassou, M. Devoret, J. M. Delrieu, and N. S. Sullivan, Phys. Rev. B **30**, 2940 (1984); J. Low Temp. Phys. **59**, 45 (1985).
[18]M. E. R. Bernier and J. H. Hetherington, Phys. Rev. B **39**, 11 285 (1989).
[19]I. Iwasa and H. Suzuki, J. Low Temp. Phys. **62**, 1 (1986).
[20]I. Iwasa, J. Phys. Soc. Jpn. **56**, 1635 (1987).
[21]D. S. Greywall, Phys. Rev. B **15**, 2604 (1977); **16**, 5129 (1977).
[22]J. R. Beamish and J. P. Franck, Phys. Rev. B **26**, 6104 (1982); **28**, 1419 (1983).
[23]C. Ebner and C. C. Sung, Phys. Rev. A **5**, 2625 (1972).
[24]M. Bloom, Physica **23**, 767 (1957).
[25]G. W. Smith and C. F. Squire, Phys. Rev. **111**, 188 (1958).
[26]W. P. A. Hass, N. J. Poulis, and J. J. W. Borleffs, Physica **27**, 1037 (1961).
[27]F. Weinhaus and H. Meyer, Phys. Rev. B **7**, 2974 (1973).
[28]R. F. Buzerak, M. Chan, and H. Meyer, J. Low Temp. Phys. **28**, 415 (1977).
[29]D. Zhou, C. M. Edwards, and N. S. Sullivan, Phys. Rev. Lett. **62**, 1528 (1989).
[30]D. Zhou, M. Rall, N. S. Sullivan, C. M. Edwards, and J. P. Brison, Solid State Commun. **72**, 657 (1989).
[31]N. S. Sullivan, D. Zhou, M. Rall, and C. M. Edwards, Phys. Lett. A **138**, 329 (1989).
[32]L. H. Nosanow, Phys. Rev. **146**, 120 (1966); J. H. Hetherington, W. J. Mullin, and L. H. Nosanow, *ibid.* **154**, 175 (1967).
[33]J. P. Hansen and D. Levesque, Phys. Rev. **165**, 293 (1968).
[34]A. Abragam and M. Goldman, in *Nuclear Magnetism: Order and Disorder* (Oxford University Press, Oxford, 1982), Chap. 3.
[35]R. P. Giffard, W. S. Truscott, and J. Halton, J. Low Temp. Phys. **4**, 153 (1971).
[36]A. B. Harris, Phys. Rev. B **2**, 3495 (1970).
[37]A. Abragam, in *Principles of Nuclear Magnetism* (Clarendon, Oxford, 1961), Chap. X.

[38]S. Washburn, R. Schweizer, and H. Meyer, J. Low Temp. Phys. **40**, 1036 (1980); R. Schwizer, S. Washburn, and H. Meyer, Phys. Rev. Lett. **40**, 1036 (1978).
[39]I. Yu, J. Low Temp. Phys. **40**, 625 (1985).
[40]Model CGR-1-3000, Lake Shore Cryotronics, Columbus, OH 43229.
[41]L. Fredericks, C. M. Edwards, and N. S. Sullivan (unpublished).
[42]D. P. Locke, J. Low Temp. Phys. **32**, 159 (1978).
[43]M. G. Richards, J. Pope, and A. Widom, Phys. Rev. Lett. **29**, 708 (1972); **37**, 760 (1976).
[44]A. R. Allen, M. G. Richards, and J. Schratter, J. Low Temp. Phys. **47**, 290 (1982).
[45]J. M. Delrieu and N. S. Sullivan, Phys. Rev. B **23**, 3197 (1981).
[46]V. N. Grigoriev, B. N. Esselson, V. A. Mikheev, V. A. Slusarev, M. S. Strzhemechny, and Y. E. Schulman, J. Low Temp. Phys. **13**, 1965 (1973).